ANALYSIS OF FLUID-STRUCTURE INTERACTION IN ABDOMINAL AORTIC ANEURYSM WITH HIGH AND NORMAL BLOOD PRESSURE

Badreddin Giuma s.k[1], Kahar Osman[1] and Mohamed Rafiq Abdul Kadir[1,2]

[1]Faculty of Mechanical Engineering, Universiti Teknologi Malaysia, 81310 UTM Skudai, Malaysia
[2]Biomechanics & Tissue Engineering Group, Faculty of Biomedical Engineering and Health Science, Universiti Teknologi Malaysia, 81310 UTM Skudai, Malaysia.
Email: bbaadre@gmial.com

ABSTRACT

In this study, we investigate the behavior of the pulsatile blood flow in an actual Abdominal Aortic Aneurysm derived from the computed tomography (CT) scan images. The human blood is assumed to behave as non-Newtonian fluid. Fluid-structure interaction (FSI) technique was used to predict the displacement and stresses on the wall. The objective of this work is to study the effect of hypertensive blood pressure and the wall shear stress (WSS) since hypertension is reported to be a risk factor in rupture of aneurysms. The numerical prediction shows that the transient behavior of the interaction under hypertensive blood pressure is significantly different from that under normal blood pressure. The peak wall stress, peak WSS and peak deformation occur shortly after systolic peak pressure. The location of maximum WSS is not where the pressure is the highest but rather where the pressure gradient is the largest.

1. INTRODUCTION

Abdominal aortic aneurysm (AAA) is a bulge in the wall of the abdominal aorta that may rupture if not surgically treated, which is associated with some mortality and morbidity. Ideally, this surgery is performed only when the risk of aneurysm rupture is high. Currently, there is no reliable criterion to predict this risk on an individual basis (Scotti and Finol 2007). The decision to electively repair an AAA is widely based on the ''maximum diameter criterion''; i.e., when the extended reach a certain size (5.5 cm), it is thought that the risk of rupture requires repair (Vorp 2007), but rupture also occurs in smaller aneurysms while some of those considered large will not rupture. Therefore the maximum diameter criterion may not be an accurate parameter to predict the risk of rupture and the needs for surgical treatment (van Dam, Dams et al. 2008).

AAA rupture is a mechanical failure when the stress developed in the aneurysm wall exceeds the yield strength of the material. The stress increases because the blood pressure grows the wall outwards, and this growth is resisted and balanced by forces (stresses) in the wall. The engineering stress analysis of simple axisymmetric shapes shows that the stress in both directions is directly proportional to the diameter, and inversely proportional to the thickness of the aneurysm wall. Thus, the stresses increase as the diameter increases, but decrease as the thickness increases (Speelman, Bosboom et al.). Hence it is logical to relate risk of rupture to aneurysm size, and hemodynamic factors like wall stress and blood pressure. However, because AAA have complicated asymmetric shapes, the relationship is more complex, and the stress in an AAA will depend on the entire geometry. It is for this reason that recent improvements in the knowledge of AAA geometry, coupled with the advances in imaging technique have focused on relating the rupture risk to AAA geometry and resultant wall stress rather than diameter alone (Raghavan, Kratzberg et al. 2006). Recently it has been shown that Fluid/Structure Interaction (FSI) can give a prediction of stress values in individual aneurysms using geometry derived from CT scan data (Wolters, Rutten et al. 2005).

In this work the real abdominal aortic aneurysm AAA was simulated using fluid structure interaction with high and normal pressure and the results were compared, to investigate the effect of hypertensive blood pressure on abdominal aortic aneurysm AAA.

2. METHODS

2.1 AAA GEOMETRY

The patient-specific geometry used in this study is derived from a computed tomograpy (CT) scans which were imported into image processing software (MIMICS). The wall thickness of AAA was marked manually for 100 slices then 3D model was calculated fig. 1 shows Slice with outline of aneurysm (A,B, and C), and (D) is the 3D model of AAA. The resultant surface data was exported into AMIRA(3D visualization and modeling system) software for the final stage of the reconstruction as shown in fig. 2.

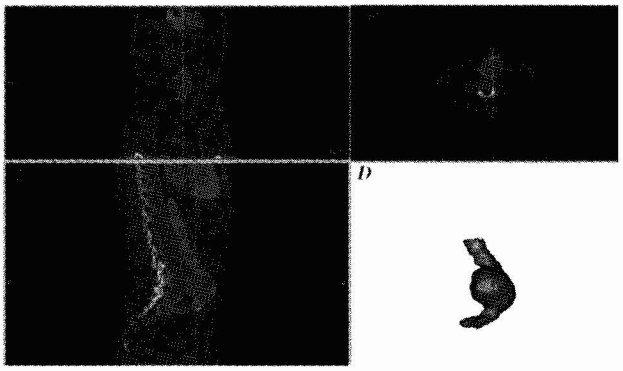

Fig. 1 Slice with outline of aneurysm (A,B, and C), and (D) is the 3D model of AAA

Fig. 2 the final Geometry of AAA generated from AMIRA software

The two software were utilized for the numerical simulation of FSI between the wall and lumen. EFD.Lab was used for the simulation of fluid while MARC MENTAT was used for the simulation of solid.

2.2 Governing Equations and Boundary Conditions for the Fluid Domain

The blood velocity and pressure distribution in AAA are computed by solving the continuity and Navier-Stokes equations with the assumptions of homogenous, incompressible, and non-Newtonian flow. The transient three-dimensional incompressible fluid flow, the governing equations in tensor (or comma) notation, following Einstein's repeated index convention (Khanafer, Bull et al. 2009), are:

(Continuity) $$u_{i,i} = 0.0 \qquad (1)$$

(Momentum)

$$\rho \frac{\partial u_i}{\partial t} + \rho u_i u_{i,j} = -p_{,i} + \tau_{ij,j} + \rho f_i \quad \text{in } \Gamma^F(t) \qquad (2)$$

(Stress tensor) $$\tau_{ij} = \eta \dot{\gamma}_{ij} \qquad (3)$$

where u_i is the component of the velocity in the i direction, p_i is the pressure scalar, ρ is the fluid density, f_i is the body force at time t per unite mass which is considered negligible, as an AAA patient lies on a hospital bed during CT scans (Khanafer, Bull et al. 2009) $\Gamma^F(t)$ is the moving spatial domain upon which the fluid is described, $\dot{\gamma}_{ij} = \left(\frac{\partial u_i}{\partial x_j} + \frac{\partial u_j}{\partial x_i}\right)$ is the shear rate tensor, according to the Power Law model:

$$\eta = m \dot{\gamma}_{ij}^{\,n-1} \qquad (4)$$

Where the specific values for m and n can be found in (Johnston, Johnston et al. 2006)

EFD.Lab was used to solve the flow equations. For the flow field computations, the AAA wall was assumed rigid and blood was modeled as an incompressible, non-Newtonian fluid(Power Law model) with a density of 1003 kg/m^3, maximum dynamic viscosity 0.012171 Pa*s, minimum dynamic viscosity 0.003038269 Pa*s and power law index 0.7991. The boundary of the fluid domain is divided into two regions Γ^F_{inlet} and Γ^F_{outlet} as shown in fig. 3. The boundary conditions on the inlet region Γ^F_{inlet} is a pulsatile velocity profile (Scotti and Finol 2007) which is shown in fig. 4a, and the time dependent normal traction (due to luminal pressure) (Tayfun E. Tezduyar 2008) on the outlet region Γ^F_{outlet}, which is shown in fig 4b where the blue and red lines depict the pressure waveform for the normal blood pressure (NBP), and high blood pressure (HBP) cases, respectively. No-slip condition is applied at the wall.

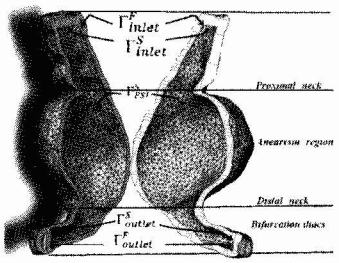

Fig. 3 schematics of AAA with the boundary conditions for fluid and solid domains

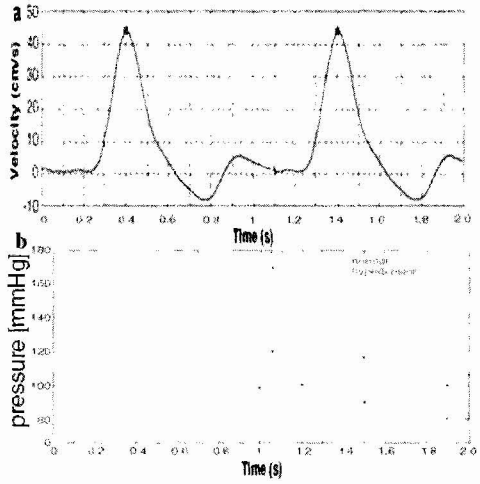

Fig. 4 Transient behavior of the boundary conditions

2.3 Governing Equations and Boundary Conditions For the Solid Domain

The governing equation for the solid domain is the momentum conservation (Li, Kleinstreuer et al. 2005) given by Eq.5

$$\nabla . \tau_s + f_s^B = \rho_s \ddot{d}_s \qquad (5)$$

ρ_s is the AAA wall density, τ_s is the solid stress tensor, f_s^B are the boby forces per unit volume, and $\ddot{d}_s$ is the local acceleration of the solid.

MARC MENTAT was used to solve the momentum equations, the AAA wall was modeled as an isotropic, linear, elastic solid with a density $\rho_s = 2.0$ g/cm^3, a Young's Modulus E=2.7 MPa and a Poisson's ratio $\upsilon = 0.45$ [13]. the boundary of the solid domain is divided into inlet Γ^s_{inlet}, outlet Γ^s_{outlet} and the fluid-structure interface Γ^s_{fsi} regions, as shown in fig 3. The boundary conditions impose zero translation on the ends Γ^s_{inlet} and Γ^s_{outlet} the pressure at the interface of the fluid domain is specified as a the time varying boundary condition for the interface of solid domain Γ^s_{fsi}.

3. RESULTS AND DISCUSSION

Figures 5, 6, and 7 show the pressure and velocity distribution along the three lines, two beside the wall (1 and 3) and the third one in the center of the AAA for both the HBP and NBP cases at end diastole, peak systole, late systole, end systole, and mid diastole in the second period. The pressure distribution along the three lines for HBP is larger than for NBP at all time and the maximum pressure occurs at peak systole for both cases and also the large pressure gradient. The velocity along the three lines reach the maximum at peak systole for both cases (HBP&NBP). There is only a slight difference between the velocity distribution of HBP and NBP cases.

The compaision of pressure distribuition at peak systole for HBP between the three lines (1,2, and 3) is shown in figure 8, the highest pressure distribution appears in line one and the largest pressure gradient appears in line three .

Figure 9 depict the transient behavior of the wall shear stress (WSS) obtained from FSI simulation for HBP and NBP cases. The maximum WSS magnitude for HBP is approximately 14% higher than NBP.The maximum WSS occurs immediately after the peak systole (1.5s) for the both cases, NBP and the HBP. The maximum WSS location is indicated with arrow in figure 9. In all cases the maximum WSS location is near the distal neck and proximal neck and has a low magnitude at the center of the aneurysm walls. The location of the highest WSS shown in figure 9 is not where the wall pressure is the highest (see figure 8) but rather where the pressure gradient is the largest. For HBP case at peak systole, a large pressure gradient occurs at the proximal neck and distal neck as evident from figure 8, where is the location of the maximum WSS

The maximal principal wall stress distributions of the AAA are presented for both HBP and NBP cases in the fig 10. The maximum principal stress occurs at the peak systole and near distal neck as indicated with the arrow. The comparison of the principal stress distribution for HBP is considerably large. For NBP case the maximum principal stress at peak systole is 8% lower than for HBP case. Although the maximal principal wall stress distribution on the inner wall differs from that on the outer wall, the two are closely related. Either aside or opposite to stress concentrations on one side of the wall, on the other side similar or complementary concentrations occur (see figure 11)

Figure 12 shows the displacement distributions for both HBP and NBP at end diastole, peak systole, end systole, and mid diastole in the second period. the maximum displacement occurs at the peak systole for the both cases, The magnitude of the maximum displacement for HBP case at peak systole is 12% higher than for NBP case. In both cases the aneurysm exhibits a rotating motion (illustrated with the arrows in the figure). there are differences in the displacement between the anterior and exterior wall to show this, four lines drawn, two in the interior wall and two in exterior wall as shown in figure 13.

CONCLUSIONS

In this work we have computed the FSI of AAA under pulsatile laminar flow conditions with high and normal blood pressures to investigate the effect of hypertension on the AAA. our results show that hypertensive blood pressure causes significant changes in the WSS

distribution and the stress distribution in the aneurysmal wall. The peak wall stress, peak WSS and peak deformation occur shortly after systolic peak pressure. The high wall shear stress occurs near the distal neck and proximal neck while a low and almost constant shear stress is typical at the center of the aneurysm region The location of maximum WSS is not where the pressure is highest but rater where the pressure gradient is largest.

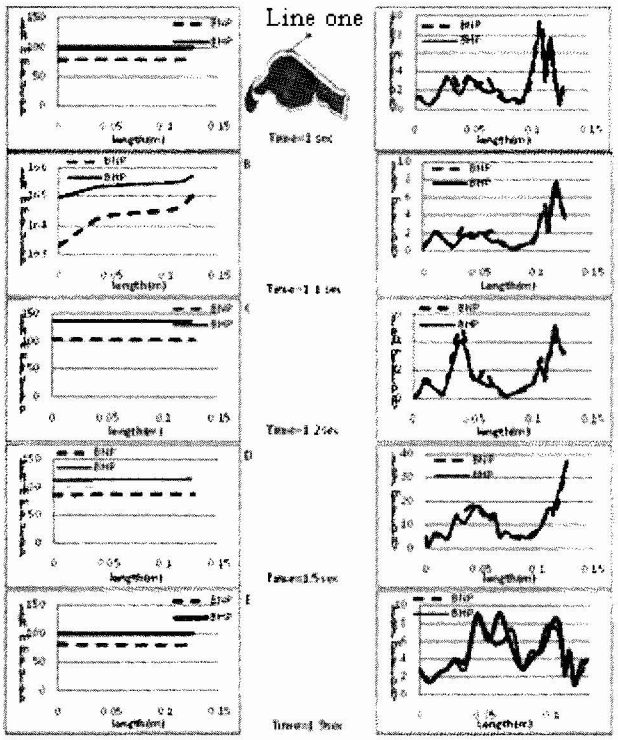

Fig. 5 Distribution of the pressure and velocity at normal and hypertensive (NBP&HBP) along line one at (A) t=1 sec (B) t=1.1 sec (C) t=1.2 sec (D) t=1.5 sec (E) t=1.9 sec

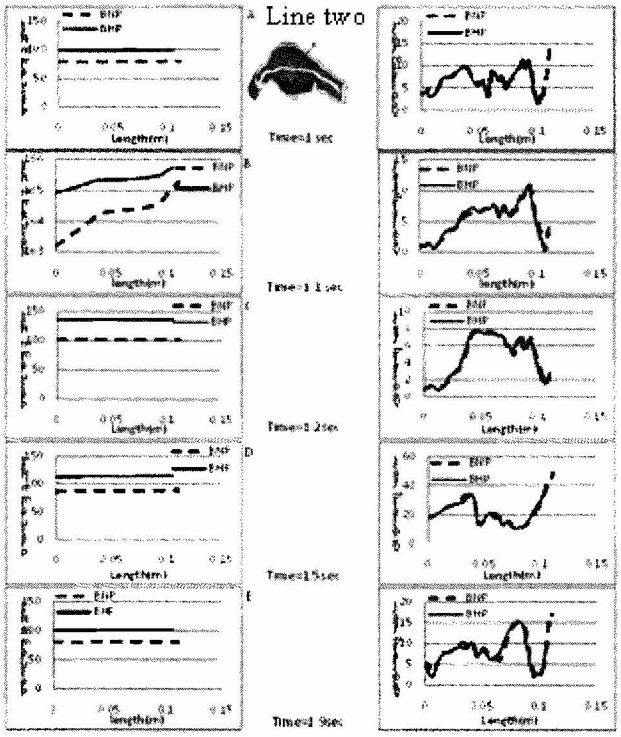

Fig. 6 Distribution of the pressure and velocity at normal and hypertensive (BNP&BHP) along line two at (A) t=1 sec (B) t=1.1 sec (C) t=1.2 sec (D) t=1.5 sec (E) t=1.9 sec

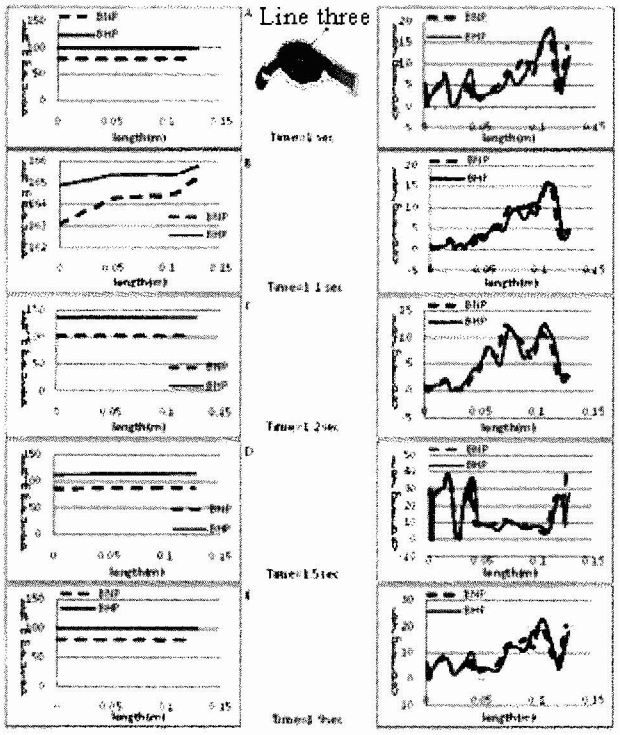

Fig. 7 Distribution of the pressure and velocity at normal and hypertensive (BNP&BHP) along line three at (A) t=1 sec (B) t=1.1 sec (C) t=1.2 sec (D) t=1.5 sec (E) t=1.9 sec

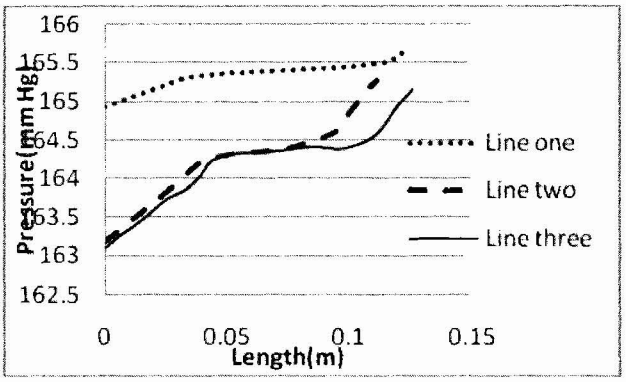

Figure. 8 Distribution of pressure(HBP) at peak systole (t=1.1 sec) along the three sketches

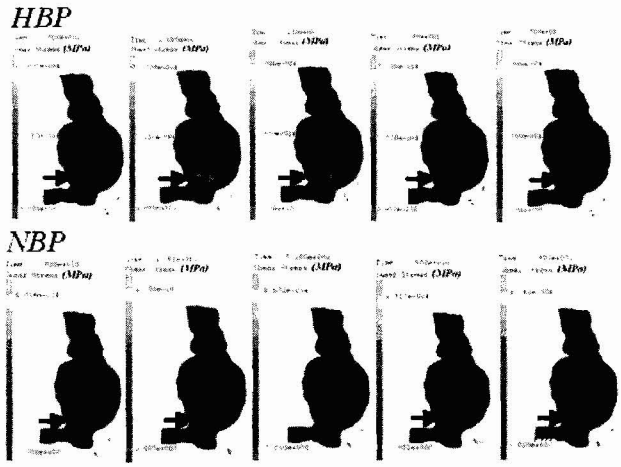

Fig. 9 instantaneous WSS distributions

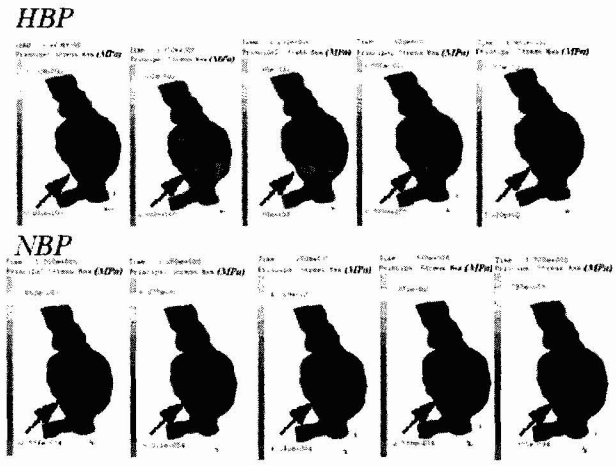

Fig. 10 instantaneous maximal principal wall stress distributions

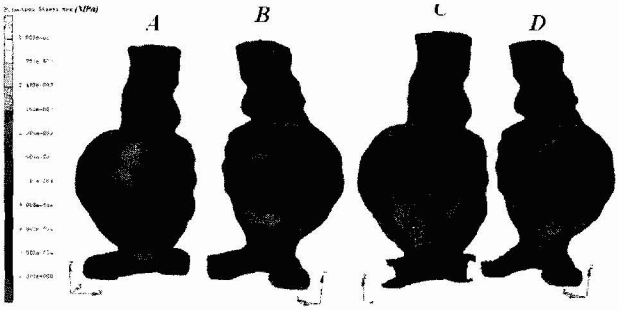

Fig. 11 Maximal principalwall stress on the deformed geometry at peak-systole for HBP: anterior/exterior (a); posterior/exterior (b); posterior/interior (c); anterior/interior
(d).

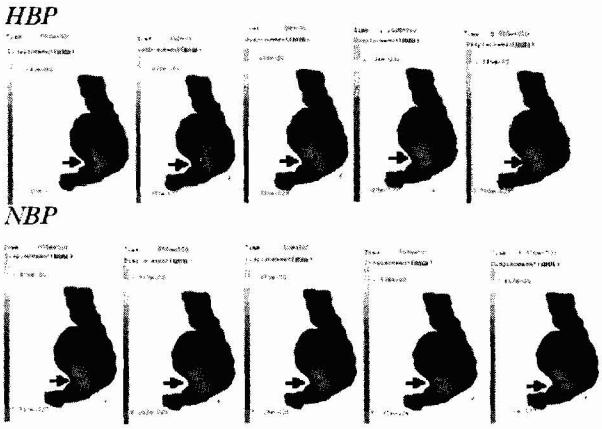

Fig 12 Instantaneous displacement distribution

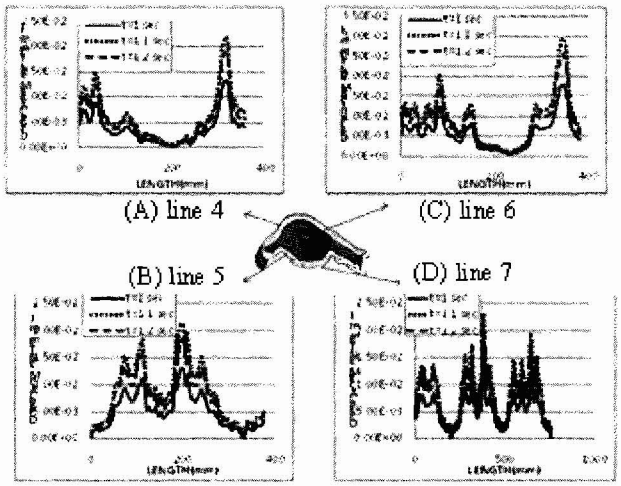

Figure 13 Displacement for the FSI analysis at different time periodic(t=1,1.1,1.2 sec) for two interior lines(5, 6) and two exterior lines(4, 6)

REFERENCES

Johnston, B. M., P. R. Johnston, et al. (2006). "Non-Newtonian blood flow in human right coronary arteries: Transient simulations." Journal of Biomechanics 39(6): 1116-1128.

Khanafer, K. M., J. L. Bull, et al. (2009). "Fluid-structure interaction of turbulent pulsatile flow within a flexible wall axisymmetric aortic aneurysm model." European Journal of Mechanics - B/Fluids 28(1): 88-102.

Li, Z., C. Kleinstreuer, et al. (2005). "Computational analysis of biomechanical contributors to possible endovascular graft failure." Biomechanics and Modeling in Mechanobiology 4(4): 221-234.

Raghavan, M. L., J. Kratzberg, et al. (2006). "Regional distribution of wall thickness and failure properties of human abdominal aortic aneurysm." Journal of Biomechanics 39(16): 3010-3016.

Scotti, C. M. and E. A. Finol (2007). "Compliant biomechanics of abdominal aortic aneurysms: A fluid-structure interaction study." Computers & Structures 85(11-14): 1097-1113.

Speelman, L., E. M. H. Bosboom, et al. "Patient-Specific AAA Wall Stress Analysis: 99-Percentile Versus Peak Stress." European Journal of Vascular and Endovascular Surgery In Press, Corrected Proof.

Tayfun E. Tezduyar, S. S. M. S. B. S. C. (2008). "Arterial fluid mechanics modeling with the stabilized space-time fluid-structure interaction technique." International Journal for Numerical Methods in Fluids 57(5): 601-629.

van Dam, E., S. Dams, et al. (2008). "Non-linear viscoelastic behavior of abdominal aortic aneurysm thrombus." Biomechanics and Modeling in Mechanobiology 7(2): 127-137.

Vorp, D. A. (2007). "Biomechanics of abdominal aortic aneurysm." Journal of Biomechanics 40(9): 1887-1902.

Wolters, B. J. B. M., M. C. M. Rutten, et al. (2005). "A patient-specific computational model of fluid-structure interaction in abdominal aortic aneurysms." Medical Engineering & Physics 27(10): 871-883.